



NASA-CR-204469

AIAA 91-0060

Internally Mounted

**Thin-Liquid-Film Skin-Friction Meter--
Comparison with Floating Element Method
With and Without Pressure Gradient**

**Jeffrey Seto and Hans G. Hornung
California Institute of Technology
Pasadena, CA**

29th Aerospace Sciences Meeting

January 7-10, 1991/Reno, Nevada

INTERNALLY MOUNTED THIN-LIQUID-FILM SKIN-FRICTION METER-- COMPARISON WITH FLOATING ELEMENT METHOD WITH AND WITHOUT PRESSURE GRADIENT.

Jeffrey Seto* and Hans Hornung**
Graduate Aeronautical Laboratories
California Institute of Technology
Pasadena, CA 91125

Abstract

A new, robust oil film skin friction meter was designed and constructed. This enables skin friction measurements remotely and from within the model, as well as avoiding the need to know the location of the leading edge of the film. The instrument was tested by comparing measurements with those given by a floating element gage in a zero pressure gradient flat plate turbulent boundary layer. Both instruments agreed satisfactorily with the well-known curve for this case. Significant discrepancies between the two instruments were observed in the case of adverse and favorable pressure gradients. The discrepancies were of opposite sign for opposite-sign pressure gradients as is consistent with the error expected from floating-element gages. Additional confidence in the oil film technique is supplied by the good agreement of the behavior of the film profile with predictions from lubrication theory.

Nomenclature

A = cross sectional area of duct
 c_f = local skin friction coefficient, τ/q
 dp/dx = external flow pressure gradient
 g = gravitational acceleration
 n = oil index of refraction
 q = free-stream dynamic pressure
 Re = Reynolds number
 t = time
 x = distance from oil film leading edge
 y = oil thickness
 ϵ = pressure gradient and gravity correction parameter
 λ = laser wavelength
 μ = oil viscosity
 ν = oil kinematic viscosity
 ρ = oil density
 τ = local skin friction

1. Introduction

In much of aerodynamic testing and research, one of the most important quantities is the skin friction. It is also one of the most difficult quantities to measure. The following three types of measurement techniques characterize the difficulties.

Direct measurement of the force due to skin friction over a small finite area is usually referred to as the "floating element method", because an element of the body surface is isolated from the rest of the surface and allowed to move under the action of the skin friction force, so that a known restoring force may be applied to return it to its null position. Difficulties associated with this method include, the problem of isolating the skin friction from other forces such as that due to pressure gradient; the elaborate nature of the instrument; and the fact that only a temporal mean force may be measured. The method has the advantage of not relying on any theoretical arguments and assumptions.

This is not the case with the so-called hot film sensors, which measure the temperature change of a heated element on the surface caused by the cooling due to the flow. The use of hot film sensors for skin friction measurements relies on the Reynolds analogy between the heat transfer rate and skin friction, and is therefore to be treated with care, especially in compressible or strongly three-dimensional flows. It is therefore also necessary to calibrate such sensors extensively. They do have the very significant advantage of being capable of measuring unsteady skin friction forces.

The third method of importance is that using the deformation rate of a liquid film placed on the surface of the body under the action of the gas flow over it. This was shown by Tanner and Blows (1976) to be interpretable directly to give the skin friction. Extensive work using optical interferometry from outside of the body include the papers by Tanner (1976, 1977abc, 1979), Tanner and Blows, Monson and Higuchi (1981), Murphy and Westphal (1986), and Westphal et al. (1986). The idea to use the technique from within the body was first suggested by Hornung and Bütetfisch (1986) and was applied to laminar flat plate flow and viscosity measurement by Marquez (1989). The liquid film technique requires no calibration (except the knowledge of the viscosity of the liquid). It is very robust and could easily be applied in flight experiments. It does not resolve temporal changes in the skin friction. Measurements using the liquid film technique from within the body so far have relied on the measurement of the film thickness at a single point and deduced the slope of the film from the assumption that its leading edge position is known. The method is capable of considerable refinement, in particular, the uncertainty introduced by this assumption may be eliminated.

The present work sets out to test a relatively robust version of the liquid film skin friction meter that can be operated entirely from within the body against a floating element skin

* Graduate Student, Department of Aeronautics.

** Clarence L. Johnson Professor of Aeronautics and Director, GALCIT.

friction meter. The flow chosen is that over a flat plate in subsonic flow at sufficiently high Reynolds number to obtain a turbulent boundary layer. The arrangement is such that the two instruments are located at two spanwise locations and may be interchanged. The relative sensitivity of the techniques to pressure gradients is also of particular interest.

2. Theory and Instrument

The concept behind the thin film technique is that the surface shear stress can be deduced from the rate of deformation of a thin oil film based upon lubrication theory. As discussed by Tanner and Blows, in instances where the oil film is thin compared to its length, the surface curvature is small, and the flow is unaffected by the presence of the film, the shear stress is the primary force on the film. Subsequently, characteristic profiles based on lubrication theory can be derived which relate the flow conditions and the shear stress. Thus, by finding the means to study the deformation of the thin oil film as a function of time, it is possible to accurately determine the skin friction.

For the specific case of this experiment, the characteristic film profile for constant shear stress, zero pressure gradient two-dimensional flow is

$$y = \frac{\mu x}{\tau t}, \quad (1)$$

where y is the film thickness, μ is the viscosity, τ is the shear stress, t is the time, and x is the distance from the leading edge of the film. A schematic of the profile is shown in Figure 1.

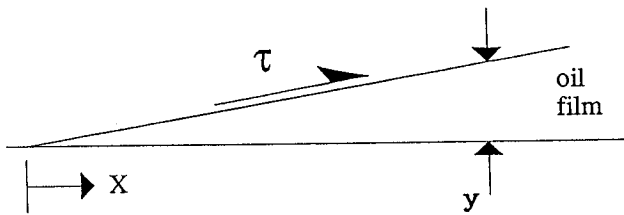


Figure 1. Oil Film Profile.

In conditions where a small pressure gradient is present in the flow ($\frac{y}{\tau} \frac{dp}{dx}$ assumed small), the profile of Equation 1 is perturbed such that it obeys the form of Equation 2.

$$y = \frac{\mu x}{\tau t} \left[\frac{1}{1 + \epsilon} \right], \quad (2)$$

where

$$\epsilon = \frac{1}{3} \frac{y}{\tau} \frac{dp}{dx} + \frac{2}{3} \frac{\mu}{t} \int \frac{1}{p_0} \frac{dp}{\tau^2}. \quad (3)$$

Thus, as time increases and the film thickness decreases, the profile will converge to that of the linear profile of a zero pressure gradient condition. More importantly, it was noted by Tanner and Blows, that near the leading edge, the profiles quickly become linear and show no effect of the pressure gradient. This fact will be referred to in the experimental results with pressure gradient.

Much of the evolution of this technique has come in the manner in which the oil film has been studied. Since the early work of Tanner and Blows, the thickness of the oil film has been monitored by interferometry using the reflections of coherent light from the air-oil interface and from the oil-surface interface which combine to give an interference pattern. Tanner and Blows took interferograms of the entire film at successive times in order to study the film as a function of both space and time. Their work validated the assumptions given in their paper and led to Tanner's later work in two-dimensional and three-dimensional flows, separated flows, and on flat and curved surfaces. Although this was successful, the method was time-consuming and inconvenient. Thus Tanner (1977a) began focusing the laser beam down to a single point and used it to study the change in thickness at that point. Combining this information with a physical measurement of the leading edge distance, Tanner used equation 1 to determine the shear stress acting on the thin film. Although it is more convenient than the previous method, this technique did not account for changes in the leading edge distance over the course of the experiment and still required optical access through the tunnel walls. Monson and Higuchi (1981) implemented a dual beam system which monitored the change in film thickness at two locations thus enabling the determination of the shear stress without requiring a measurement of the leading edge distance. The present work extends this concept by expanding the laser beam and monitoring the interference pattern with a linear CCD array. Rather than analyzing distinct points within the profile, the arrangement allows for the entire profile to be studied as a function of time. This set-up will be especially valuable for use in studying profiles which are not linear, such as might occur in flows with pressure gradients. In addition to accounting for the possible leading edge creep, the set-up provides for greater accuracy and can detect deviations from the expected profiles. Previously such deviations would be relegated as uncertainties or mysteries.

A schematic of the instrument is shown in Figure 2. The light originates from a 5 mW He-Ne laser which is focused onto a fiber optic cable using a fiber optic coupler. The cable can be used to transport light to a remote testing location, which eliminates the need for access through tunnel windows and rigid alignment constraints. The expanding beam from the other end of the fiber is collimated using a plano-convex lens which produces a beam of light approximately 4 mm in diameter. A beamsplitter cube serves both as a portion of the

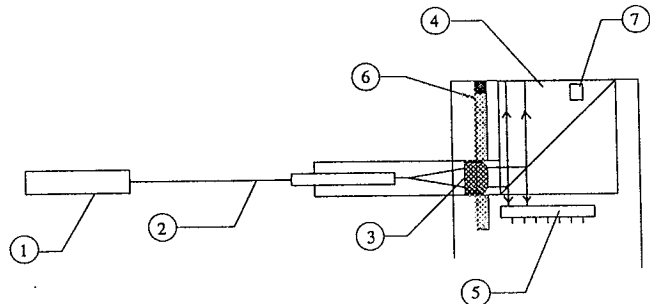


Figure 2. Thin Liquid Film Skin Friction Meter 1) He-Ne laser; 2) Fiber-optic cable; 3) Plano-convex lens; 4) Beamsplitter cube; 5) CCD linear array; 6) Oil delivery system; 7) Thermocouple.

plate surface and also as the means to direct the light towards the surface and the oil. The oil is applied to the surface via a porous material placed just ahead of the beamsplitter. The interference pattern is recorded on a linear CCD array placed under the beamsplitter. This signal is recorded at discrete times by a Nicolet digital storage oscilloscope for use in the data analysis. The temperature of the instrument is monitored by a thermocouple attached to its side. The laser, computer, oil injection device, and oscilloscope can all be kept outside and away from the tunnel, while all the other components are housed in a cylindrical package for ease of operation and installation. The important elements of this scheme are its remote operation, complete analysis of the film, and self-contained convenient package.

For all the experiments, the interference pattern is monitored by the CCD array. A sample of the output of the array is shown in Figure 3. The array gives a direct spatial representation of the interference pattern as exhibited by the local maxima and minima of light intensity corresponding to the bright and dark fringes of the pattern. Each successive maximum or minimum corresponds to an increase in overall path length of one wavelength, which means that the light has traveled an additional wavelength in comparison to the previous maximum or minimum. Thus the entire profile can be deduced from an analysis of the extrema. Figure 4 is a plot of the spacing between the dark fringes for the pattern shown in Figure 3. The constant fringe spacing or spatial frequency of the signal clearly demonstrates the linear nature of the profile, representing the effect of the shear stress acting on the film in the absence of a pressure gradient. This type of analysis was also valuable in monitoring any deviations from the expected profile.

One problem encountered in the aforementioned analysis is that beside the two reflections from the air-oil and oil-surface interfaces, a third reflection of light occurs at the back of the

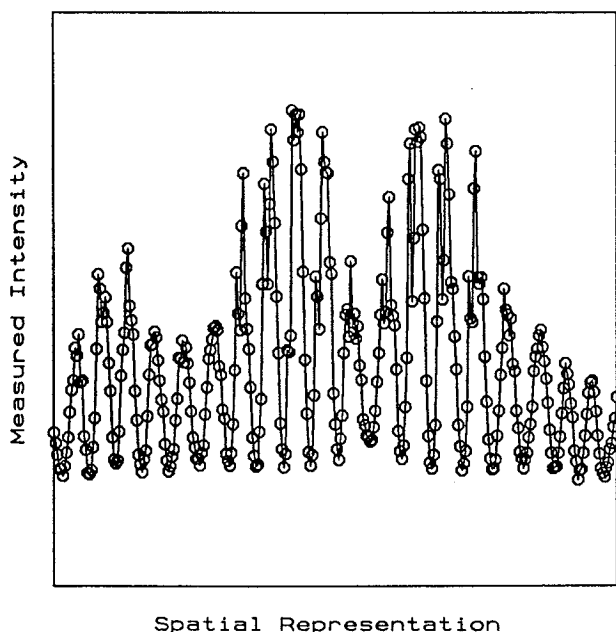


Figure 3. Spatial fringe pattern as recorded by the CCD array. The circles represent values recorded by individual sensors of the array.

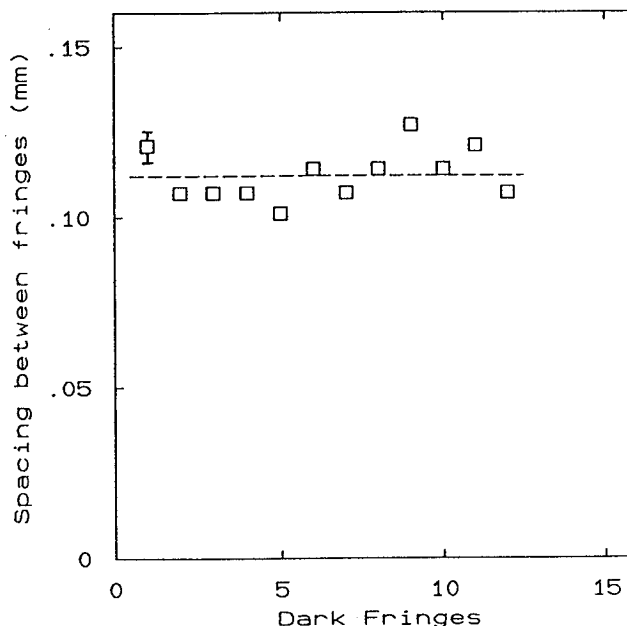


Figure 4. Fringe spacing corresponding to the pattern of Figure 3.

beamsplitter and contributes to the pattern. Thus an interference pattern could be detected before any oil was applied to the surface. This resulted in a constant frequency offset. The measured slope in the experiments is a linear combination of the actual oil film slope and the offset slope. The prism offset was measured before and after each set of experiments and subtracted from the measured CCD profile to obtain the actual film slope. The offset value remained constant throughout the runs, as expected. This offset frequency directly affected the minimum film slope which could be measured. As long as the frequency of the oil film pattern is greater than that of the offset pattern, a proper measurement of the oil film could be obtained. However, when both frequencies were comparable, the signals would adversely interfere such that the desired signal was obscured. In future modifications to the apparatus, the beamsplitter will be coated to remove this third reflection.

3. Experiments

The instrument was used to measure the skin friction distribution along a flat plate on which a major part of the boundary layer is turbulent. The flat plate spans the entire test section of the low-speed Merrill wind tunnel at GALCIT. The cross section of the tunnel is 4 ft. by 3.5 ft.. The flat plate is 8 ft. in length and is designed such that the skin friction instrument can be placed at any one of five different longitudinal stations. The experiment is augmented by the use of a Kistler Skin Friction Balance System (floating element) which was placed side-by-side with the oil film instrument at each station to provide an important and convenient method of comparing the two techniques.

Four groups of experiments with zero pressure gradient were conducted with each taking place at a different longitudinal station. At each station, the oil film instrument and the surface element gage were placed on opposite sides of the centerline. The minimum time needed to store each

waveform, combined with the minimum slope constraint, defines both the required oil viscosity and the speed range possible at each location. For reasons given by Tanner (1977b), Dow Corning 200 silicon oils were chosen for the experiments because of their low vapor pressure, chemical inertness, and low temperature coefficient of viscosity. Nominal viscosities of 50 cs, 100 cs, and 200 cs were used. A range of velocities from 7 m/s to 30 m/s was used at each location to obtain a full range of Reynolds numbers. The combination of the longitudinal stations and the different speeds allows for the study of the boundary layer over a wide range of Reynolds numbers. Disturbances created by the upstream plugs for the station holes not in use caused early transition so that all of the comparisons take place with skin friction measurements of a turbulent boundary layer. The early transition is not a problem in these experiments, since the aim here is to compare instruments.

4. Results and Discussion

4.1 Zero pressure gradient

The first comparison of the two instruments was made in the case of a zero-pressure gradient turbulent boundary layer. This also affords the possibility of comparison with the well-known values for this case.

The method of monitoring the changing slope of the oil film was selected as the most effective means of determining the skin friction. The method does not depend on a measurement of the leading edge distance and also does not need a constant recording of the profile, but does require the storage and analysis of the profile at designated times. This type of analysis is based on equation 4 which describes the relation between the film slope and the time:

$$\frac{dx}{dy} = \frac{\tau}{\mu} (t_m + t_0). \quad (4)$$

Here t_m is the time measured during the experiment, and t_0 is the time corresponding to the initial oil film condition. For each stored interference profile, the oil film slope was measured and the corresponding time was recorded. Based on Equation 4, the inverse of the slope was plotted against the measured time, and a linear curve fit to the data was performed. The initial time, t_0 was thus determined as was the constant of proportionality (τ/μ). The details of the calculations are described in the Appendix. Figure 5 displays these results for several values of shear stress as measured by the floating element device. The data points lie very close to the line, thus demonstrating the validity of the theory. Qualitatively, it is seen that as the shear stress increases, the slope of the film decreases more rapidly.

The skin friction coefficients were computed for both the oil film and the floating element gage. Figure 6 is a compilation of the values for the experiments at each location. This figure illustrates the accuracy to which the oil film meter measured the skin friction in a turbulent boundary layer based on the comparison with the floating element gage. Nearly all the oil film values lie within 7% of the corresponding floating element reading. The values also closely agree with the local turbulent skin friction coefficient for a smooth flat plate.

The most noticeable deviation is seen at a Reynolds number of approximately 7×10^5 . Upon initial discovery of this

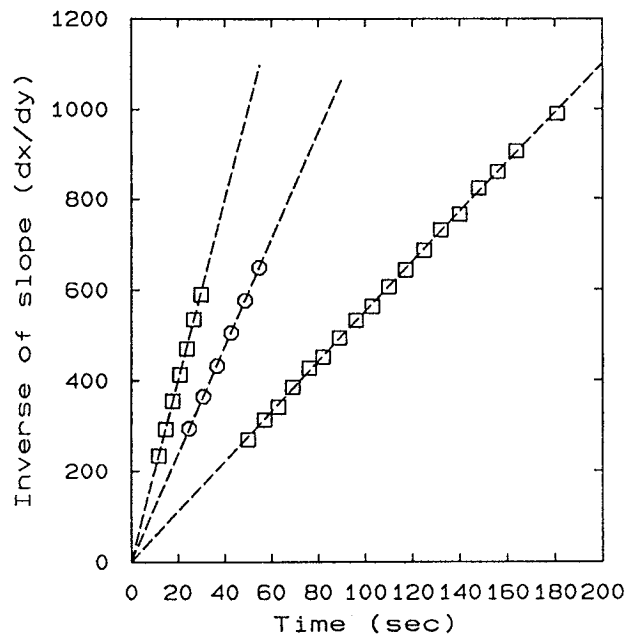


Figure 5. Plot used to determine shear stress. Zero pressure gradient case. The points are obtained from the oil film measurements. Their slope gives the shear stress.

deviation, the spanwise location of the two instruments was exchanged to investigate whether the discrepancy was due to a spanwise variation. The result of this test was negative. A possible reason for this may be the slight pressure variation along the length of the plate as shown by Figure 7, or another factor present in the flow at this condition. Nevertheless, the results shown in Figure 6 validate the ability of the oil film meter to measure skin friction accurately over the flat plate at a wide range of Reynolds numbers.

4.2 Non-zero pressure gradients

As stated previously, the case of a non-zero pressure gradient is of special interest to experimenters. Therefore, the wind tunnel test section was modified to allow for skin friction measurements in both an adverse and a favorable gradient. As shown in Figure 8, a ramp was installed along the length of the test section such that a linear area contraction and expansion is obtained. An area ratio of $A_t/A_{inlet} = 0.6$ is achieved two-thirds of the plate distance from the leading edge. A series of experiments were performed in both the adverse and favorable gradient regions of the flow.

Using the area contraction shown in Figure 5, tests were conducted to compare the skin friction readings of the oil film meter and the floating element gage in the presence of both an adverse and a favorable pressure gradient. Figure 9 shows the pressure distribution along the flat plate caused by the contraction. Upstream of the throat, the flow accelerates causing a drop in the static pressure of the flow, and consequently a favorable pressure gradient ($dp/dx < 0$). Conversely, the expansion downstream of the throat decelerates the flow creating an adverse pressure gradient ($dp/dx > 0$).

Based on lubrication theory, the effect of the pressure gradient on the motion of the oil film is described by Eq. 2

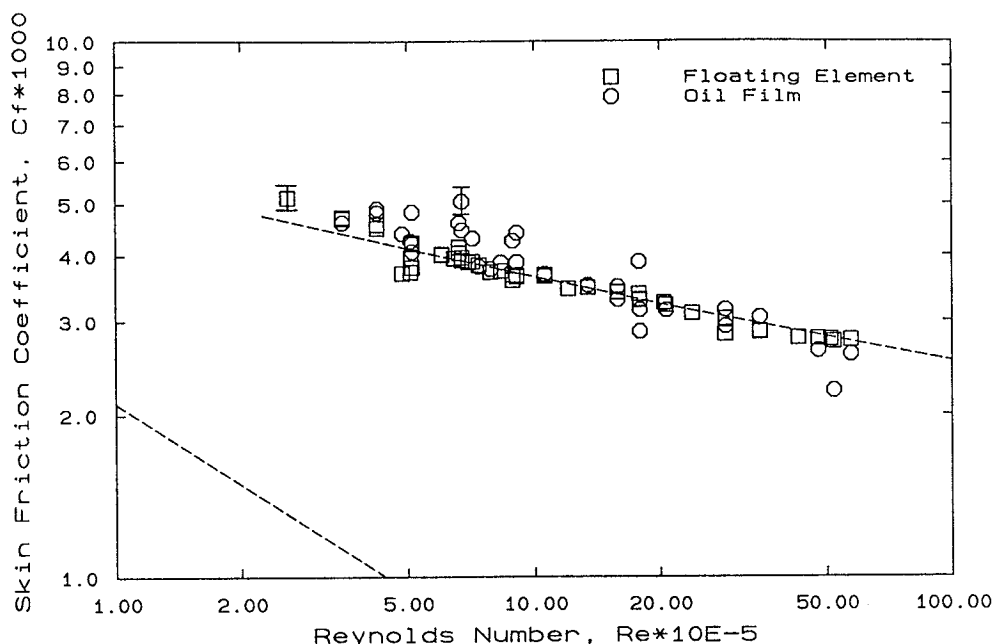


Figure 6. Comparison of zero pressure gradient skin friction measurements by floating element and oil film gage.

provided that the pressure gradient is small compared to the shear stress divided by film thickness. As the film becomes thinner, the gradient has much less effect on the film motion, and near the leading edge of the film, where the film is thin after a very short time, the effect of the pressure gradient becomes negligible and thus the true shear stress can be accurately determined by a similar analysis to that of the zero pressure gradient case. For both the adverse and favorable gradients, the CCD array permitted the analysis of the linear portion of the film, such that the shear stress could be determined in the same manner as previously. Much greater attention was paid to the nature of the profile because fluctuations in the flow caused deviations from the predicted theory. Figure 10 shows a plot of the inverse of the slope versus the time for two cases of dp/dx . As in the previous analysis, the correspondence to a linear relationship between the two variables demonstrates the negligible effect the pressure gradient has on the film by the time that measurements are taken. (A pressure-gradient-dominated condition would result in a parabolic film profile.)

This type of analysis performed well in both pressure gradient conditions. Figure 11 shows the skin friction coefficients plotted versus flow speed for the case of favorable pressure gradient in the flow (upstream portion of the flat plate). A significant difference in skin friction values as measured by the two instruments is now apparent. The oil film meter values are all greater than the corresponding floating element readings by an average of 70%.

Figure 12 shows the skin friction plotted versus Reynolds number for the case of the adverse gradient on the downstream part of the plate. Again, the difference between the two devices is large, but the sign of the difference has changed. This fact is consistent throughout all the experiments.

As presented in the Introduction, one of the drawbacks of the floating element device is its performance in a pressure

gradient. The action of the pressure differences on the central element will cause additional forces not due to the shear stress. The sign of the error of a floating element gage due to pressure gradient is a complex combination of flow through the gap and normal force distribution over the area of the element. Depending on the construction of the gage the sign of the error may be the same or opposite to the sign of the pressure gradient (see Allen, 1976). However, for a given gage, the sign of the error always changes with the sign of the pressure gradient. The results of the comparison between the two devices indicate that the assumption that the oil film measurement is correct is consistent with this expectation.

The behavior of the oil film profile with time shown in Figure 10 for the pressure gradient case confirms the lubrication theory very satisfactorily. This gives added confidence in the use of the oil film gage in pressure gradients. Nevertheless, a more extensive investigation of the technique in flows with pressure gradients and in complex turbulent flows is needed.

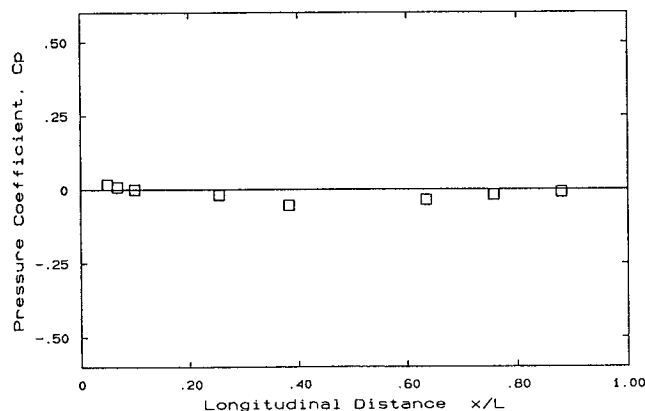


Figure 7. Pressure distribution in the case of nominally zero pressure gradient.

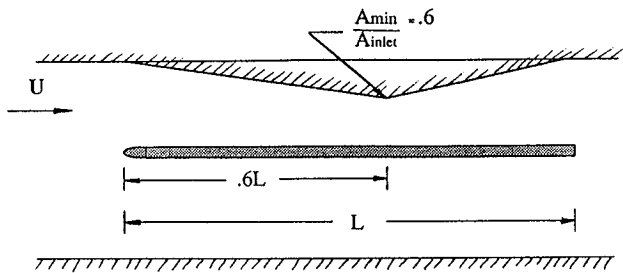


Figure 8. Experimental setup for pressure gradient case.

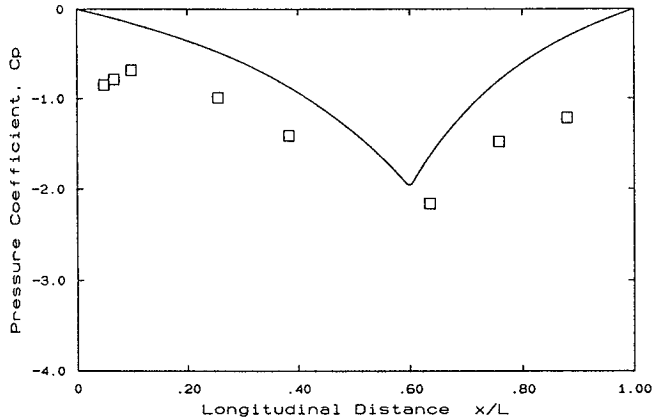


Figure 9. Pressure distribution on the plate with the test section as sketched in Figure 8. Symbol: measurement; line: inviscid quasi-one-dimensional calculation.

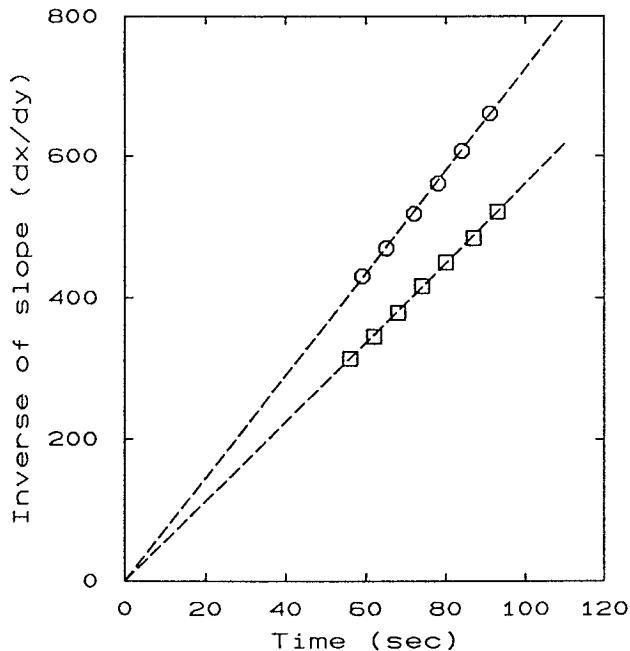


Figure 10. Plot used to determine shear stress in adverse (circles) and favorable (squares) pressure gradient flow. Note that the points still lie on good straight lines.

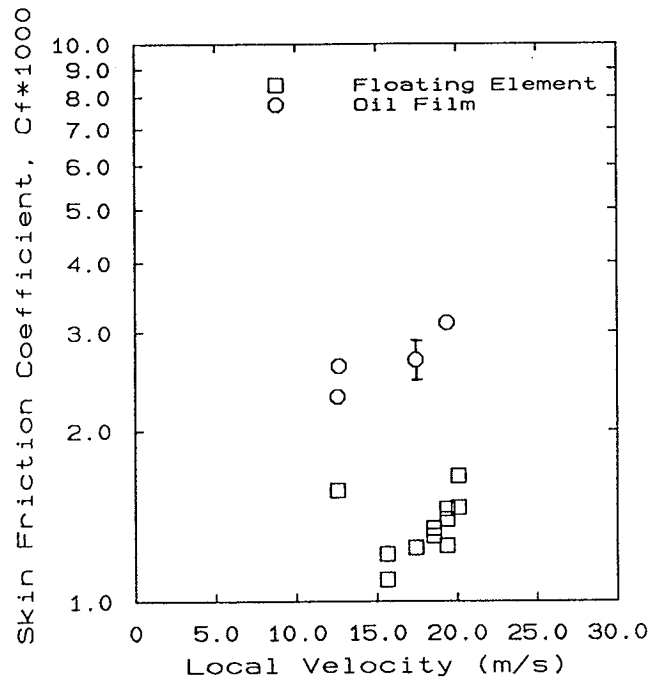


Figure 11. Skin friction measurements in the favorable pressure gradient (at 3.25 ft from leading edge).

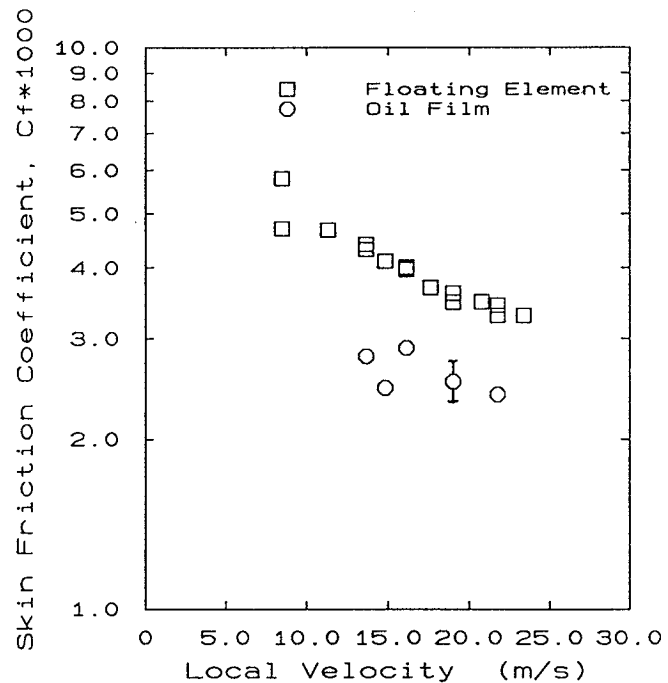


Figure 12. Skin friction measurements in the adverse pressure gradient (at 6.5 ft from the leading edge).

5. Conclusion

Experiments in positive, zero and negative pressure gradient turbulent boundary layer flows have been conducted, in which skin friction measurements with a floating element and with a thin-oil-film meter have compared. In the case of zero pressure gradient the agreement between the two

instruments and with the well-known smooth flat plate curve is satisfactory. In the case of positive and negative pressure gradient the discrepancy between the two instruments is significant and of opposite sign. The agreement of the behavior of the film profile with lubrication theory gives confidence in the oil film meter.

The oil film meter used in these experiments incorporates special features including robustness, remote operation and measurement of the complete film profile at any time.

6. References

- [1] Allen, J. M. 1976 Systematic study of error sources in supersonic skin-friction balance measurements. *NASA-TN-D-8291*.
- [2] Tanner, L. H. and Blows, L. G. 1976 A study of the motion of oil films on surfaces in air flow, with application to the measurement of skin friction, *J. Phys. E: Sci. Instrum.* **9**, 194-202.
- [3] Tanner, L. H. and Kulkarni, V. G. 1976 The viscosity balance method of skin friction measurement: further developments including applications to three-dimensional flow, *J. Phys. E: Sci. Instrum.* **9**, 1114-21.
- [4] Tanner, L. H. 1977a A skin friction meter, using the viscosity balance principle, suitable for use with flat or curved metal surfaces, *J. Phys. E: Sci. Instrum.* **10**, 278-84.
- [5] Tanner, L. H. 1977b A comparison of the viscosity balance and preston tube methods of skin friction measurement, *J. Phys. E: Sci. Instrum.* **10**, 627-32.
- [6] Tanner, L. H. 1977c A more accurate viscosity balance measurement of the variation of skin friction with Reynolds number, for comparison with Preston tubes, *J. Phys. E: Sci. Instrum.* **10**, 843.
- [7] Tanner, L. H. 1979 Skin friction measurements by viscosity balance in air and water flows, *J. Phys. E: Sci. Instrum.* **12**, 610-9.
- [8] Monson, D. J. and Higuchi, H. 1981 Skin friction measurements by a new non-intrusive double laser beam-oil viscosity balance technique, *AIAA J.* **19**, 739-44.
- [9] Westphal, R. V., Bachalo, W. D. and Houser, M. 1986 Improved skin friction interferometer, *NASA TM* **8**, 8216.
- [10] Murphy, J. A. and Westphal, R. V. 1986 The laser interferometer skin-friction meter: a numerical and experimental study, *J. Phys. E: Sci. Instrument.* **19**, 744-751.
- [11] Hornung, H. and Bütetisch, K.-A. 1986 Verfahren und Vorrichtung zur Bestimmung der Wandschubspannung oder der Viskosität von Flüssigkeiten an Modellen und anderen umströmten Körpern. European Patent Application No. 86105414.6 Sheet 86/44.
- [12] Marquez Olivares, J. 1989 Absolutbestimmung der Wandschubspannung mit Hilfe eines Interferometers, *DFVLR-FB* **89-13**.

Acknowledgment

This work is funded by Grant No. NAG 2-621 from NASA Ames (Dr. Dennis Koga).

Appendix: Skin Friction Calculation

The method of calculating the skin friction from the instrument output will now be discussed for completeness. The actual output of the CCD array and associated hardware is a time varying voltage output corresponding to the light intensity of the individual pixels which are discharged at a fixed frequency. The triggered output can be fed to an oscilloscope or similar device to give a stable signal such as in Figure 3. The signal allows for the determination of the time to pass from one dark fringe to another (dt/dF). This can be easily related to the actual film slope by Equation 5

$$\frac{dy}{dx} = \frac{dF}{dt} \frac{dt}{dx} \frac{dy}{dF}, \quad (5)$$

where dt/dx is the relation between the rate of CCD output and the physical distance on the array itself. The term dy/dF is the actual change in film thickness corresponding to the distance from one fringe extremum to another. As the light passed perpendicular to the surface, dy/dF is of the form

$$\frac{dy}{dF} = \frac{\lambda}{2n}, \quad (6)$$

where λ is the wavelength of the laser (He-Ne: $\lambda = 632.8$ nm) and n is the index of refraction of the silicon oil.

Once dy/dx is known, the inverse of the slope dx/dy is plotted against the time corresponding to each slope and a linear curve fit is performed based on Equation 4 to give the terms (τ/μ) and t_0 . The shear stress, τ , is then determined by calculating the viscosity of the silicon oil based on the temperature of the instrument. In further modifications to the apparatus, a thin metal film will be deposited on the prism surface to more accurately determine the oil temperature. This ambiguity should introduce uncertainties of only 1 or 2%.